ISSN 2663-1563 Vol. 5, Issue 2: 43-51, DOI: 10.25236/AJAGE.2023.050208

Study on the Spatial-Temporal Evolution of Land Use and Its Thermal Environmental Effects in Chengdu

Jiahao Yu*, Chuliang Xin, Xiaojing Feng

College of Architecture and Urban-Rural Planning, Sichuan Agricultural University, Chengdu, 611800, China
**Corresponding author: 201908211@stu.sicau.edu.cn*

Abstract: *With the accelerating urbanization process, the urban land use structure has changed, and urban environmental and resource problems have become increasingly prominent. Among them, the urban heat island effect has seriously affected the sustainable development of society. Therefore, from the perspective of mitigating the urban heat island effect, this study uses two phases of remote sensing images of Chengdu in 2002 and 2019 as the main data. Using the methods of supervised land use classification and surface temperature inversion, the spatial and temporal changes and characteristics of land use and surface temperature in the central urban area of Chengdu are analyzed. The effects of different land use types on the surface temperature are also explored to investigate their thermal environmental effects. The main research results are as follows: (1) the area of construction land in the central urban area of Chengdu increased greatly from 2002-2019, and the proportion changed from 12.4% to 41.2%; the area of cultivated land and forest land decreased significantly. (2) The high-temperature area was mainly concentrated in the central region from 2002 to 2019, and the area was increasingly expanded; the low-temperature area shifted from the original northwest region to the eastern and southern regions. (3) Land use change was significantly correlated with the thermal environment. Surface temperature was negatively correlated with NDBI and positively correlated with NDBI.*

Keywords: *Land Use Evolution, Land Surface Temperature, Spatial-Temporal Characteristics, Chengdu City*

1. Introduction

The rapid urbanization process has led to the expansion of urban areas and dramatic changes in land use patterns. The change of land use type has caused serious impact on economic and social sustainable development and ecological security. The expansion of cities has occupied a large amount of arable land and forest land, changed the nature of the original urban substrate [1], and seriously affected the heat balance of the land surface [2]. At the same time, due to the influence of human activities and other factors, the urban surface temperature keeps rising and the urban heat island effect becomes increasingly serious [3]. The urban heat island effect can change the ecological environment of cities, leading to frequent high temperature disasters and accelerated urban energy consumption [4]. Numerous studies have shown that land use/cover change is the main driver of the urban thermal environment [5-7]. It is important to study and mitigate the urban heat island effect in terms of land use type changes.

In recent years, due to the advantages of remote sensing data coverage, multi-scale, multi-temporal phase, and economy, more scholars tend to use remote sensing technology to dynamically monitor surface land use conditions and invert surface temperature [8]. Imhoff et al. combined MODIS and TM remote sensing images to extract impervious surface and surface radiation temperature information of urban study [9]. Xu Hanqiu studied the influence of surface parameter changes on the urban thermal environment and conducted a quantitative study on the relationship between ground radiation temperature and parameters such as vegetation cover, water bodies and impervious surface [10]. Sultana et al. used Landsat series data to quantitatively analyze land use changes and their spatial relationship with surface temperature in 10 major cities in India [11].

Since the planning of Tianfu New Area was carried out in Chengdu, its construction land, population density, roads, and building density have greatly increased, which has intensified the urban heat island effect, and the future development of Chengdu may face a huge heat wave impact. Therefore, in this paper, a supervised land use classification and surface temperature inversion are performed for the central

ISSN 2663-1563 Vol. 5, Issue 2: 43-51, DOI: 10.25236/AJAGE.2023.050208

urban area of Chengdu City using two phases of remote sensing images in 2002 and 2019. Focusing on the relationship between land use and thermal environment in Chengdu city, we explore the countermeasures to mitigate the heat island effect in Chengdu city. To provide scientific support for rational urban land use, and thermal environment management.

2. Study Area and Data

2.1 Overview of the study area

Chengdu is located in the central part of Sichuan Province, and the central city area identified in the "Chengdu National Central City Industrial Development Conference" was selected as the study area (Figure 1). Chengdu city has a subtropical monsoon climate with abundant heat and rainfall. The average annual temperature is 15.7-17.7°C, the total annual precipitation is 798.3-1541.0 mm, and the average annual sunshine hours are 685.5-1002.9 h. The city is crisscrossed by rivers, with main streams such as Minjiang and Tuojiang flowing through it. And the land types are diverse, with 94.2% of the usable land area.

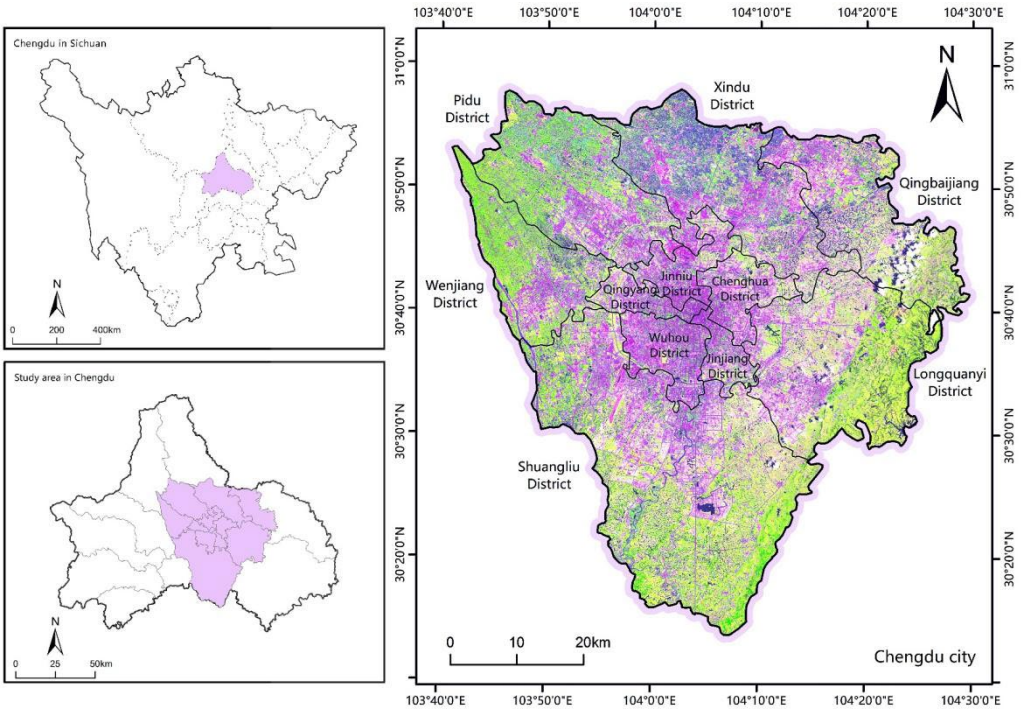

Figure 1: Location of the Study Area

2.2 Data source and processing

Two phases of remote sensing imagery based on the study area were derived from the geospatial data cloud (http://www.gscloud.cn/). Landsat4-5 TM images were dated June 25, 2002, and Landsat8 OLI_TIRS images were dated August 11, 2019. The image clouds were all less than 2, which met the requirements of surface temperature inversion. The administrative vector boundary of Chengdu City was obtained from the National Geographic Information Resources Catalogue Service (http://www.webmap.cn/). The pre-processing operations such as radiometric calibration, atmospheric correction, and cropping were all done in ENVI 5.3. The supervised classification used the maximum likelihood classification method to classify the land use types into 6 major categories: construction land, forest land, grass land, Water area, construction land and unused land. The overall accuracies of the obtained classifications were all above 90%, and the Kappa coefficients were all greater than 0.88.

ISSN 2663-1563 Vol. 5, Issue 2: 43-51, DOI: 10.25236/AJAGE.2023.050208

3. Research Methods

3.1 Surface temperature inversion

The current surface temperature inversion process applies the radiative transfer equation (RTE) method, also known as the atmospheric correction method [12]. The radiant brightness B(T_s) of a blackbody can be obtained from the radiative transfer equation. The equation is as follows:

$$B(T_s) = [L_\lambda - L_\uparrow - \tau(1-\varepsilon)L_\downarrow] / \tau \cdot \varepsilon \quad (1)$$

In equation (1), B(T_s)—the value of the surface radiant brightness of the blackbody at TS temperature; L_λ—the value of the thermal infrared radiant brightness; ε—the surface radiance; τ—the atmospheric transmittance in the thermal infrared band; $L_\uparrow$, $L_\downarrow$—the atmospheric upward and downward radiant brightness. Where, τ, $L_\uparrow$ and $L_\downarrow$ are available through the official website of NASA (http://atmcorr.gsfc.nasa.gov/). The true surface temperature T_s is derived from the inverse function of Planck's law. equation is as follows:

$$T_s = K_2 / \ln(K_1 / B(T_s) + 1) \quad (2)$$

In equation (2), K_1=607.76 $W \cdot m^{-2} \cdot sr^{-1} \cdot \mu m^{-1}$ and K_2=1260.56K for the TM satellite sensor, and K_1=774.89 $W \cdot m^{-2} \cdot sr^{-1} \cdot \mu m^{-1}$ and K_2=1321.08K for the TIRS satellite sensor.

3.2 Surface temperature classification

The mean-standard deviation method was used to classify the temperature classes based on the degree of deviation of surface temperature relative to the mean temperature. The temperature is first normalized. The formula is:

$$T_i = (T_{i0} - T_{min})/(T_{max} - T_{min}) \quad (3)$$

In equation (3), T_i is the normalized temperature value of the i-th image element; T_{i0} is the original temperature value of the i-th image element; T_{max} and T_{min} are the maximum and minimum values of the surface temperature, respectively.

The normalized image element mean and standard deviation are used to classify the surface temperature classes into six classes: extra-high temperature zone, high temperature zone, sub-high temperature zone, medium temperature zone, sub-medium temperature zone and low temperature zone [13]. The specific division criteria are shown in Table 1.

Table 1: Surface temperature class classification standards

Temperature Level	Temperature range
Extra-high Temperature zone	$T_i > T_{mean} + T_s$
High Temperature zone	$T_{mean} + 0.5T_s < T_i \leq T_{mean} + T_s$
Sub-high Temperature zone	$T_{mean} < T_i \leq T_{mean} + 0.5T_s$
Medium Temperature zone	$T_{mean} - 0.5T_s < T_i \leq T_{mean}$
Sub-medium Temperature zone	$T_{mean} - T_s < T_i \leq T_{mean} - 0.5T_s$
Low Temperature zone	$T_i \leq T_{mean} - T_s$

Note: T_i, T_{mean} and T_s are the normalized image element values, mean and standard deviation, respectively.

3.3 Supervised classification algorithm

The maximum likelihood method is based on the waveband data of the selected sample images, which are used as a multidimensional normal distribution to construct the actual classification function. The image elements in the images of the study area are calculated and substituted into the classification function to achieve the final result of classification. Assuming that the image has n bands, the expression of the density function of the normal distribution corresponding to the type i site is:

$$P(x/G_i) = \frac{|S_i^{-1}|^{\frac{1}{2}}}{(2\pi)^{\frac{n}{2}}} exp\left[-\frac{1}{2}(x-\mu_i)^T S_i^{-1}(x-\mu_i)\right] \quad (4)$$

In equation (4), S_i—the covariance matrix of n bands of the i-th land use type.

If the land use types in the study area are divided into m categories, there are m probability distribution density functions corresponding to them, and thus the probability of each type can be calculated. As

ISSN 2663-1563 Vol. 5, Issue 2: 43-51, DOI: 10.25236/AJAGE.2023.050208

opposed to calculating the random variable x in the m categories, when the random variable x is known, the probability of category i in the m categories can be derived according to the Bayesian formula. The expression is:

$$P(G_i/x) = [P(G_i)P(x/G_i)]/P(x) \tag{5}$$

Simplifying equation (5), the final expression is:

$$P(G_i/x) = -\frac{1}{2}\ln|S_i| - \frac{1}{2}(x-\mu_i)^T {S_i}^{-1}(x-\mu_i) \tag{6}$$

In equation (6), μ_i—the mean vector, which is the mean value of the sample band features in the actual classification; the value of i is taken from 1 to 6, because the land use type in this paper is 6 categories.

4. Results and Analysis

4.1 Analysis of land use change

As can be seen from Figure 2 and Figure 3, in terms of spatial distribution, construction land from 2002 to 2019 was mainly concentrated in the core areas of the central city (Jinniu District, Wuhou District, Qingyang District, Jinjiang District, and Chenghua District). Construction land from 2002 to 2019 expanded rapidly, radiating from the center to the surrounding area, with significant changes in spatial structure. The area of construction land increased from 457.94km^2 in 2002 to 1516.52km^2 in 2019. Cultivated land had the widest distribution in 2002, mostly clustered in the north and west. It basically covered Wenjiang district, Pidu district and Xindu district. 2019 Cultivated land was greatly reduced, from 1836.41km^2 in 2002 to 1204.22km^2. The overall distribution was in broken patches, mosaic between construction land. The area of forest land is mainly distributed in Longquan Mountain Range, however, with the expansion of construction land, the area of woodland decreased year by year. 2002, the southern and eastern part of the large area of forest land, while in 2019, only the southeastern edge of the continuous forest land, the reduction of the area of 833.46km^2. Grass land and unused land accounted for a relatively small area, but the increase was large, 388.16% and 161.23% respectively. The area of water area decreased from 84.22km^2 in 2002 to 27.17km^2 in 2019.

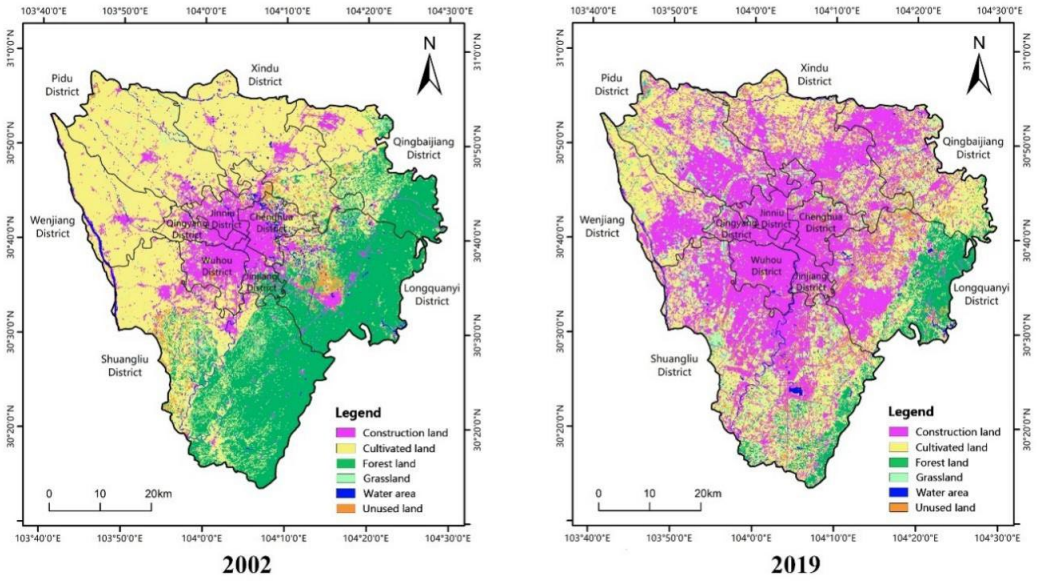

Figure 2: Land use distribution map of central urban area of Chengdu in 2002 and 2019

By comparing the distribution of land use in 2002 and 2019, it can be found that the increase in construction land was mainly converted from cultivated land, reflecting the rapid expansion of towns and cities, with a large amount of hard ground replacing farmland. Forest land was mainly transformed into cultivated land and unused land, reflecting the destruction of forest land during urban development and the degradation of the ecological quality of some cropland. The increase of grass land area reflected the effectiveness of park city construction in Chengdu in recent years, with a large increase of urban park

ISSN 2663-1563 Vol. 5, Issue 2: 43-51, DOI: 10.25236/AJAGE.2023.050208

green space.

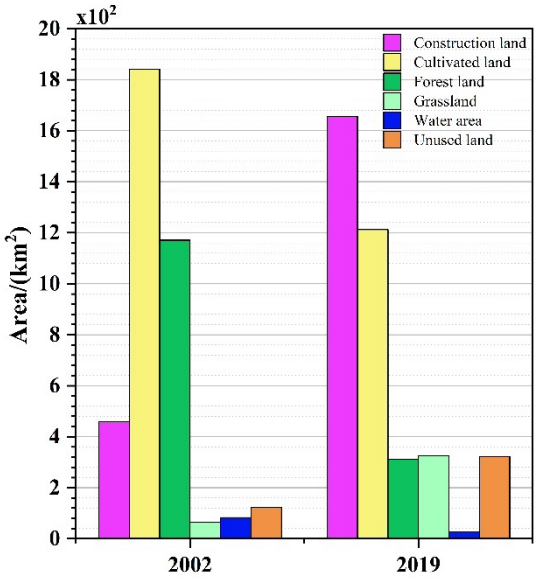

Figure 3: Histogram of land use area in the central city of Chengdu in 2002 and 2019

4.2 Analysis of surface temperature change

According to the results of temperature classification, the distribution of surface temperature levels in the study area is obtained in Figure 4. Low temperature zone was mainly distributed in the northwest area of the central city, mainly in Xindu District, Pidu District and Wenjiang District. With the growth of time, the low temperature zone shifted from the northwest region to the eastern Longquan Mountain Range region. The sub-medium temperature zone was concentrated in the northwest region from 2002 and distributed around the extra-high temperature zone in 2019. The distribution area of the medium temperature zone was larger, and in 2002 it was mainly distributed in the east and south of the central city. During 2002-2019, the medium temperature zone as a whole moves to the northwest. The change of the sub-high temperature zone was similar to that of the medium temperature zone. The high temperature zone was mainly concentrated in the eastern part of the central city in 2002, with a large proportion in Longquanyi District, and mainly distributed in the central area in 2019. The distribution of the extra-high temperature zone changed less, and is basically located in the core area of the central city. By 2019, the extra-high temperature zone had spread to the surrounding area compared with 2002.

The area occupied by different temperature zones is shown in Figure. 5. In 2002, the area of medium temperature zone was significant, amounting to 1143.43 km^2. The area of other temperature zones was less different, among which the area of high temperature zone and extra-high temperature zone were 436.36 km^2 and 471.13 km^2 respectively. In 2019, it mainly showed sub-medium temperature zone and medium temperature zone, and the area of both was basically the same. The area of the extra-high temperature zone increased to 612.67 km^2 in 2019. The area of the sub-medium temperature zone reached 863.70 km^2 in 2019, which was a large increase. The area of low temperature zone also increased slightly. The overall change in temperature from 2002 to 2019 showed a decrease in the medium temperature zone and an increase in the sub-medium zone and extra-high temperature zone, and the regional temperature difference was gradually becoming larger.

ISSN 2663-1563 Vol. 5, Issue 2: 43-51, DOI: 10.25236/AJAGE.2023.050208

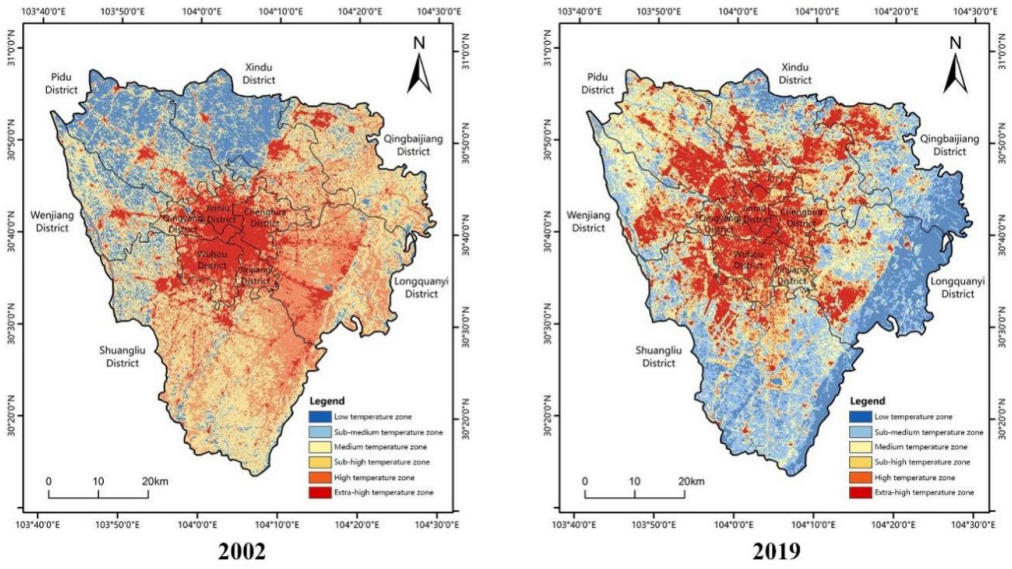

Figure 4: Temperature class distribution in the central city of Chengdu in 2002 and 2019

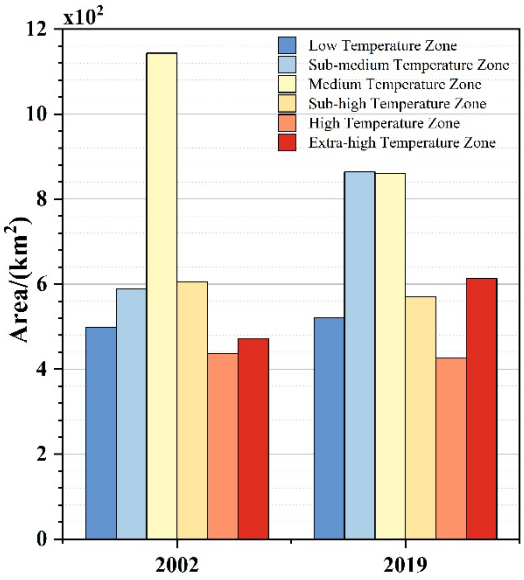

Figure 5: Histogram of area of different temperature zones in the central city of Chengdu in 2002 and 2019

4.3 Analysis of the thermal environmental effects of land use change

4.3.1 Relationships between land use types in response to the thermal environment

In order to study the response relationship of land use types to urban thermal environment, each temperature zoning in different land use types was analyzed. The spatial distribution of urban heat island classes and land use status data were overlaid and analyzed in ArcGIS10.5, and the specific results are shown in Tables 2 and 3 below.

Construction land was distributed in a large area of extra high temperature area, the overall temperature was high. The cultivated land showed mainly low temperature zone, sub-medium temperature zone as well as medium temperature zone in surface temperature zoning. Forest land mainly exhibited medium temperature zone, sub-high temperature zone as well as high temperature zone in 2002, and decreased in area in 2019, exhibiting low temperature zone and sub-medium temperature zone. Grass land were mainly represented as medium temperature zones in 2002 and increased in area in 2019, with the proportion of sub-medium zone exceeding that of medium temperature zone. Water area was smaller, and the area of each temperature partition was more evenly distributed in 2002, but in 2019 it mainly showed the low

ISSN 2663-1563 Vol. 5, Issue 2: 43-51, DOI: 10.25236/AJAGE.2023.050208

temperature area. The unused land mainly showed sub-high temperature zone and high temperature zone in 2002, but mainly showed medium temperature zone and sub-high temperature zone in 2019.

The extra-high temperature zone within the construction land dominated in 2002, and with the accelerated urbanization, the overall temperature of the city showed an increasing trend and the heat island range was expanding. By 2019, the overall temperature of the central city was higher, resulting in a decrease in the proportion of the extra-high temperature zone. The proportion of each temperature partition of cultivated land land did not change much, mainly because the area of cultivated land accounted for a relatively large proportion of the overall temperature change was relatively stable. Forest land dominated the low temperature zone in 2019, which showed the mitigation effect of Forest land (mainly Longquan Mountain Range) on urban heat island in the central urban area of Chengdu at this stage. Grass land accounted for a smaller proportion in the extra-high temperature zone in 2019, which also reflected the cooling effect of park green space on a local scale within the city. Water area dominated the low temperature zone, and the cooling capacity of rivers and lakes was highlighted as the overall temperature of the city rised. The nature of unused land was more easily changed, and the percentage of temperature zoning fluctuates more.

Table 2: Area of each temperature zoning under land use type in central urban area of Chengdu in 2002 (Unit: km2)

	Low Temperature zone	Sub-medium Temperature zone	Medium Temperature zone	Sub-high Temperature zone	High Temperature zone	Extra-high Temperature zone
Construction land	8.10	3.58	9.83	25.93	54.31	356.88
Cultivated land	440.54	472.89	579.23	200.37	103.61	45.14
Forest land	15.50	88.17	481.64	313.13	226.06	46.23
Grass land	6.51	9.29	30.06	13.66	5.20	1.07
Water area	27.59	12.29	16.13	14.62	8.09	4.13
Unused land	0.47	2.11	26.53	37.49	39.10	17.68

Table 3: Area of each temperature zoning under land use type in the central urban area of Chengdu in 2019 (Unit: km2)

	Low Temperature zone	Sub-medium Temperature zone	Medium Temperature zone	Sub-high Temperature zone	High Temperature zone	Extra-high Temperature zone
Construction land	42.77	107.24	230.44	334.63	355.01	586.43
Cultivated land	218.02	456.07	384.37	118.66	27.54	7.72
Forest land	210.37	85.93	13.57	1.12	0.12	0.03
Grass land	25.51	146.69	102.17	37.27	11.26	3.27
Water area	19.68	4.63	1.25	0.34	0.14	0.62
Unused Land	4.08	63.14	128.78	78.34	32.75	14.60

4.3.2 Correlation analysis of land use pattern and surface temperature

To more quantitatively analyze the driving influence of land use on urban heat island, the normalized vegetation index (NDVI), normalized building index (NDBI) and land surface temperature (LST) in the central urban area of Chengdu in 2019 were selected for correlation analysis to quantify the impact of spatial pattern of urban land use on thermal environment.

The Pearson correlation coefficient between LST and NDVI was -0.671, i.e., and the surface temperature decreased in areas with high vegetation cover in the urban center of Chengdu. The Pearson correlation coefficient between LST and NDBI was 0.686, i.e., and the surface temperature increased in areas with dense buildings in the urban center of Chengdu. The city of Chengdu was in a phase of rapid expansion in 2019, with an increasing area of construction land. The effect of buildings on temperature was more pronounced compared to vegetation, which meant that there may be a need for more parkland to regulate the regional microclimate in areas with high building density such as commercial and residential sites(Figure 6).

ISSN 2663-1563 Vol. 5, Issue 2: 43-51, DOI: 10.25236/AJAGE.2023.050208

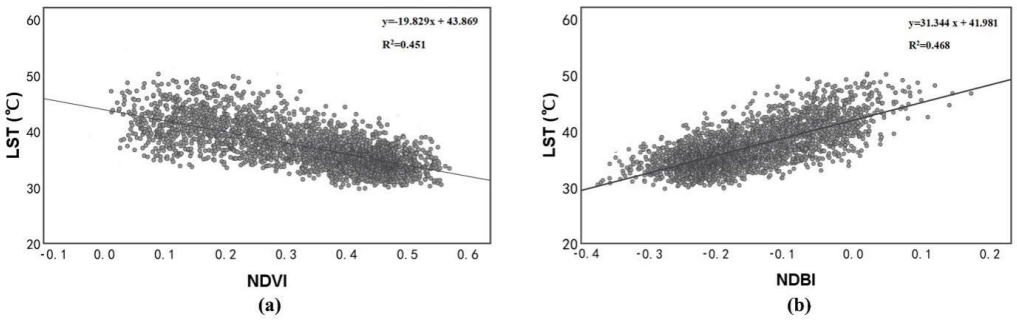

Figure 6: (a) Correlation of LST with NDVI; (b) Correlation of LST with NDBI

5. Conclusions

This study analyzed the spatial distribution and change characteristics of land use and surface thermal environment in the central city of Chengdu from 2002 to 2019 to explore the mechanism of land use structure and its change on surface temperature change. It can improve the reference basis for mitigating the urban thermal environment and improving the sustainable development of the city. The conclusions drawn from the study are as follows.

(1) The land use in the central city of Chengdu was dominated by construction land, forest land, and cultivated land. Construction land had always maintained an increasing trend during 2002-2019, with the increase area reaching 2.3 times of the initial area. The area of cultivated land and forest land gradually decreased, among which the area of forest land decreased very significantly, from 1112.65 km^2 in 2002 to 279.19 km^2 in 2019. The cultivated land was mainly converted to construction land and grass land, and the forest land was mostly converted to construction land, cultivated land and unused land.

(2) The construction land mainly showed extra-high temperature zone in surface temperature zoning. The cultivated land mainly showed low temperature zone, sub-medium temperature zone as well as medium temperature zone. The forest land shifted from medium temperature zone and sub-high temperature zone to low temperature zone and sub-medium temperature zone from 2002 to 2019. The temperature zoning of grass land had some changes, but it was still sub-medium temperature zone and medium temperature zone in general. The water area had no obvious temperature zoning in 2002, while in 2019 clearly showed a low temperature zone. The temperature zoning of unused land shifted from high temperature zone to low temperature zone from 2002 to 2019.

(3) The surface temperature had good correlation with NDVI and NDBI. The surface temperature was significantly and positively correlated with NDBI with a Pearson correlation coefficient of 0.686, which meant that the higher the building density, the higher the urban surface temperature. Surface temperature was negatively correlated with NDVI with a Pearson correlation coefficient of -0.671, which indicates that vegetation had a good effect on mitigating the heat island effect.

References

[1] Gong Adu, Chen Yunhao, Li Jing, et al. Study on Relationship between Urban Heat Island and Urban Land Use and Cover Change in Beijing [J]. Journal of Image and Graphics, 2007, (08): 1476-1482.
[2] Bian Xiaohui, Liu Yan, Ding Qianqian, et al. Response of Land Use and Cover Change to Urban Heat Island Effect in Huzhou City, Zhejiang Province [J]. Bulletin of Soil and Water Conservation, 2019, 39(03): 263-269+275.
[3] Ge Rongfeng, Wang Jingli, Zhang Lixiao, et al. Impacts of urbanization on the urban thermal environment in Beijing [J]. Acta Ecologica Sinica, 2016, 36(19): 6040-6049.
[4] Xiao Rongbo, Ouyang Zhiyuan, Li Weifeng, et al. A review of the eco-environmental consequences of urban heat islands [J]. Acta Ecologica Sinica, 2005, 25(8): 2055-2060.
[5] Pan Jinghu, Dong Leilei, Wang Nayun, et al. A multiscale study of thermal environment pattern in Lanzhou Xining agglomeration [J]. Remote Sensing for Land and Resources, 2018, 30(2): 138-146.
[6] Xie Qijiao. Analysis on characteristics and influencing factors of urban heat island effect in Wuhan [J]. Resources and Environment in Yangtze Basin, 2016, 25(3): 462-469.
[7] Ye Yu, Qin Jianxin, Hu Shunshi. Spatial-temporal evolution of urban heat island effects in Changsha City [J]. Journal of Geo-information Science, 2017, 19(4): 518-527.

ISSN 2663-1563 Vol. 5, Issue 2: 43-51, DOI: 10.25236/AJAGE.2023.050208

[8] Liu Shuang. Analysis of the Influence of Land Use Spatial Pattern on Urban Heat Island Strength in Ganzhou City [D]. Jiangxi University of Science and Technology, 2020.
[9] Marc L. Imhoff, et al. Remote sensing of the urban heat island effect across biomes in the continental USA [J]. Remote Sensing of Environment, 2009, 114(3): 504-513.
[10] Xu Hanqiu. Analysis on urban heat island effect based on the dynamics of urban surface biophysical descriptors [J]. Acta Ecologica Sinica, 2011, 31(14): 3890-3901.
[11] Sultana Sabiha, Satyanarayana A.N.V.. Urban heat island intensity during winter over metropolitan cities of India using remote-sensing techniques: impact of urbanization [J]. International Journal of Remote Sensing, 2018, 39(20): 6692-6730.
[12] Weng Qihao, Liu Hua, Lu Dengsheng. Assessing the effects of land use and land cover patterns on thermal conditions using landscape metrics in city of Indianapolis, United States [J]. Urban Ecosystems, 2007, 10(2): 203-219.
[13] Xu Mingxue, Li Jun, Yao Lei, et al. Analysis of the relationship between surface thermal environment and landscape change in Beijing-Tianjin-Hebei Region under multiple scales [J]. Journal of Xi'an University of Technology, 2021, 37(01): 43-52.